# $^{252}$Cf Plasma Desorption Mass Spectrometry in the Synthesis of Porphyrin Model Systems

**Jonathan S. Lindsey***

*Department of Chemistry, Carnegie Mellon University, 4400 Fifth Avenue, Pittsburgh, Pennsylvania 15213*

**Tanuja Chaudhary and Brian T. Chait**

*The Rockefeller University, 1230 York Avenue, New York, New York 10021*

**$^{252}$Cf plasma desorption mass spectrometry has been used in the characterization of more than 100 synthetic porphyrins ranging in mass from 614 u for tetraphenylporphyrin to over 2000 u for some porphyrin model systems. In virtually every case, $^{252}$Cf plasma desorption mass spectrometry yielded an intense ionized molecule ion [$M^{\bullet+}$ and/or $(M + H)^+$], irrespective of the groups appended to the porphyrin. The appended groups include carboxylic acids, amides, imides, chloroacetamides, Fmoc-protected amino acids, aromatic amines, nitriles, alkynes, alkenes, esters, active esters, benzyl ethers, acetals, dithioacetals, ketones, imines, phenols, quinone, hydroquinone, ferrocene, cyanine dyes, trimethylsilyl protecting groups, nitro groups, and combinations of these functionalities. Metalloporphyrins and porphyrin–porphyrin dimers are also analyzed with ease. Resolved isotopic peaks were observed for porphyrins with molecular weights below 1000, and unresolved isotopic peaks yielding average masses were observed for porphyrin compounds with higher molecular weights. The limited resolution in the higher molecular weight range does not lessen the utility of the method because the observation of the molecule ions [$M^{\bullet+}$ and/or $(M + H)^+$] provides unambiguous evidence concerning the success of the synthesis. The $^{252}$Cf plasma desorption mass spectra of porphyrins are not complicated by chemical transformations. This method is ideally suited for rapid analysis of synthetic porphyrins and provides a powerful tool for chemists engaged in the synthesis of complex organic molecules.**

## INTRODUCTION

The increasing complexity of porphyrin model systems places a premium on methods for analysis and characterization. The analytical issue in porphyrin synthesis generally is not the identification of an unknown substance, but rather the confirmation that the synthesis has proceeded as expected. Chromatographic methods such as TLC provide information concerning product homogeneity, and absorption and fluorescence spectroscopy establish the integrity of the porphyrin chromophore. These techniques require small amounts of material and are performed rapidly but are insufficient to confirm the product identity. Electronic spectra in particular provide little information about the groups appended to the meso-positions, which often constitute much of the total mass in porphyrin model systems. Indeed, the essential porphyrin framework consists of only 24 atoms (e.g., porphine, $C_{20}H_{14}N_4$, molecular mass = 310 u), but typical porphyrin model systems range in mass from 700 to above 2000 mass units. $^1$H NMR spectroscopy provides detailed structural information pertaining to the groups around the periphery of the porphyrin but often requires extensive interpretation of spectra derived from concentrated samples.

A number of different mass spectrometric methods have been applied to the analysis of porphyrinic molecules over the years.[1-3] These have focused largely on characterizing porphyrins derived from natural sources, although a few early reports concern synthetic porphyrins.[4] More recently, synthetic porphyrins have been examined by an assortment of mass spectrometric methods, including chemical ionization MS,[5] laser photodissociation tandem MS,[6] laser desorption fourier transform MS,[7] electrospray MS,[8] and fast atom bombardment MS.[9-13] The latter method has been used most extensively, and several groups have investigated the demetalation and redox reactions of metalloporphyrins that occur in the fast atom bombardment MS sample matrices.[10,11,14,15] Over the past 12 years we have utilized $^{252}$Cf plasma desorption mass spectrometry (PDMS) for the characterization of more than 100 synthetic porphyrins encompassing a variety of model system architectures. The mass spectra are collected in 1–30-min runs on a few nanomoles of the porphyrin sample. We have found that porphyrins ionize readily by $^{252}$Cf plasma desorption to form relatively stable intact molecule ions [$(M + H)^+$ and/or $M^{\bullet+}$]. Though the peripheral groups constitute the bulk of the mass in most of the porphyrin model compounds studied, the intact molecule ion was readily identifiable in nearly every case, thereby providing unambiguous confirmation of the success of the synthesis. Taken together, the universal applicability and rapid analysis make $^{252}$Cf PDMS a powerful method for assessing the outcome of syntheses of porphyrin model

* To whom correspondence should be addressed.

(1) Smith, K. M. In *Porphyrins and Metalloporphyrins*; Smith, K. M., Ed.; Elsevier: Amsterdam, 1975; pp 381–398.
(2) Budzikiewicz, H. In *The Porphyrins*; Dolphin, D., Ed.; Academic Press: New York, 1978; Vol. III, pp 395–461.
(3) Gallegos, E. J.; Sundararaman, P. *Mass Spectrom. Rev.* **1985**, *4*, 55–85.
(4) Adler, A. D.; Green, J. H.; Mautner, M. *Org. Mass Spectrom.* **1970**, *3*, 955–962. Meot-Ner, M.; Green, J. H.; Adler, A. D. *Ann. N. Y. Acad. Sci.* **1973**, *206*, 641–648. Meot-Ner, M.; Adler, A. D.; Green, J. H. *Org. Mass Spectrom.* **1974**, *9*, 72–79.
(5) Van Berkel, G. J.; Glish, G. L.; McLuckey, S. A.; Tuinman, A. A. *J. Am. Chem. Soc.* **1989**, *111*, 6027–6035.
(6) Fukuda, E. K.; Campana, J. E. *Anal. Chem.* **1985**, *57*, 949–952.
(7) Brown, R. S.; Wilkins, C. L. *Anal. Chem.* **1986**, *58*, 3196–3199.
(8) Van Berkel, G. J.; McLuckey, S. A.; Glish, G. L. *Anal. Chem.* **1991**, *63*, 1098–1109.
(9) Rubino, F. M.; Mascaro, P.; Banfi, S.; Quici, S. *Org. Mass Spectrom.* **1991**, *26*, 161–166.
(10) Naylor, S.; Lamb, J. H.; Hunter, C. A.; Cowan, J. A.; Sanders, J. K. M. *Anal. Chim. Acta* **1990**, *241*, 281–287.
(11) Musselman, B. D.; Watson, J. T.; Chang, C. K. *Org. Mass Spectrom.* **1986**, *21*, 215–219.
(12) Kurlansik, L.; Williams, T. J.; Strong, J. M.; Anderson, L. W.; Campana, J. E. *Biomed. Mass Spectrom.* **1984**, *11*, 475–481.
(13) Zhang, M. Y.; Liang, X. Y.; Chen, Y. Y.; Liang, X. G. *Anal. Chem.* **1984**, *56*, 2288–2290.
(14) Naylor, S.; Hunter, C. A.; Cowan, J. A.; Lamb, J. H.; Sanders, J. K. M. *J. Am. Chem. Soc.* **1990**, *112*, 6507–6514.
(15) Schurz, H. H.; Busch, K. L. *Energy Fuels* **1990**, *4*, 730–736.

0003-2700/92/0364-2804$03.00/0 

**Chart I. Structural Diagrams for Tetraarylporphyrins (X Substituent, See Table I) and Tetraalkylporphyrins (R Substituent, See Table I)[a]**

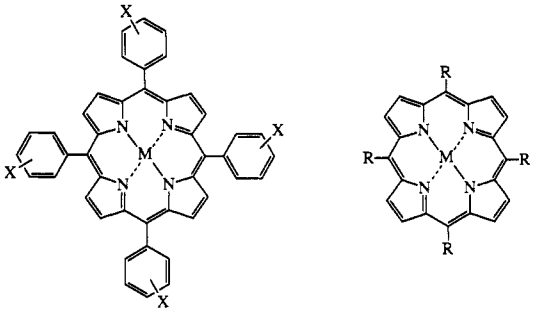


Tetra-aryl-porphyrin  Tetra-alkyl-porphyrin

[a] The porphyrins are analyzed as the free base (M = H, H) unless a metal (M, usually Zn) is indicated in the molecular formula.

compounds, i.e. recognizing when synthetic errors or incomplete reaction has occurred, or conversely, when the target material or intermediate has been correctly synthesized. In this paper we summarize the application of $^{252}Cf$ PDMS in porphyrin synthetic chemistry, thus complementing prior studies that have used this method for the characterization of chlorophyll samples.[16-18]

## EXPERIMENTAL SECTION

Porphyrin solutions were prepared at $\sim 10^{-4}$ M in solvents (such as $CH_2Cl_2$/methanol (1:1) or acetone) suitable for electrospray deposition[19] onto the mass spectrometer sample probe. Approximately 0.1 mL of the porphyrin solution was electrosprayed over the course of 5–10 min onto a 1-cm$^2$ area aluminized Mylar film. The porphyrin sample was clearly visible as a colored deposit.

The technique of $^{252}Cf$ plasma desorption mass spectrometry has been described previously.[20] The mass spectra were obtained with the Rockefeller University $^{252}Cf$ fission fragment time-of-flight mass spectrometer.[18,21] In these studies we concentrated almost exclusively on positive ion spectra. The ion acceleration voltage was 10 kV. An electrostatic particle guide maintained at −30 V with respect to the 3-m flight tube was used to increase the ion transport efficiency to the detector. The $^{252}Cf$ source with a strength of ~20 mCi yielded a flux of approximately 2000 fission fragments per second through the sample foil. The ever-present ions at $m/z$ 1 ($H^+$) and 23 ($Na^+$, from adventitious trace impurities) were used to calibrate the masses observed with the positive ion spectra.

## RESULTS

We outline our results as follows. First we present an overview of the typical spectral patterns obtained with porphyrins as a function of increasing molecular weight of appended groups. Next we describe a specific application of the method in the synthesis of a family of porphyrin cage molecules. Then we highlight issues in the characterization of diverse porphyrin compounds and model systems that, with only a few exceptions, have been synthesized using a biomimetic porphyrin reaction strategy.[22,23] Finally, we describe the characterization of porphyrin–porphyrin dimers.

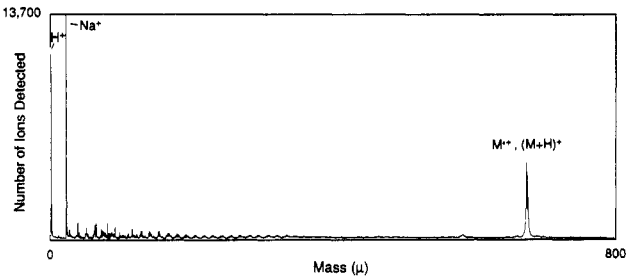


**Figure 1.** $^{252}Cf$ plasma desorption mass spectrum of *meso*-tetra(*p*-tolyl)porphyrin.

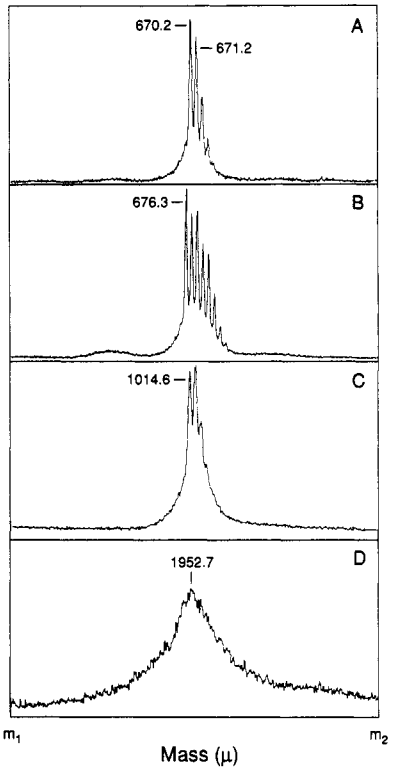


**Figure 2.** Spectra of the molecule ion region for four compounds. (A) *meso*-Tetra(*p*-tolyl)porphyrin. (B) The zinc chelate of *meso*-tetraphenylporphyrin. (C) *meso*-Tetrakis(4-(*n*-$BuO_2C$)$C_6H_4$)porphyrin. (D) *meso*-Tetrakis(4-(Fmoc-Pro-NH)$C_6H_4$)porphyrin.

**1. Typical Spectral Patterns.** The mass spectrum of *meso*-tetra(*p*-tolyl)porphyrin (4, Chart I, X = 4-$CH_3$) exhibits dominant peaks from the intact porphyrin ion (Figure 1) as well as a large number of less intense peaks arising from the fragmentation of the ionized molecule ion. The intense peaks arising from the intact porphyrin exhibit sufficient resolution to allow analysis of each of the isotopic components (Figure 2A). The lowest isotopic component[24] (A + 0) for the molecule containing $C_{48}H_{38}N_4$ ($M^{\bullet+}$) has a mass of 670.3 u and a calculated relative abundance of 57%.[25] The calculated relative abundance of the A + 1 component is 31%, which

(16) Hunt, J. E.; Macfarlane, R. D.; Katz, J. J.; Dougherty, R. C. *Proc. Natl. Acad. Sci. U.S.A.* **1980**, *77*, 1745–1748.
(17) Chait, B. T.; Field, F. H. *J. Am. Chem. Soc.* **1982**, *104*, 5519–5521.
(18) Chait, B. T.; Field, F. H. *J. Am. Chem. Soc.* **1984**, *106*, 1931–1938.
(19) McNeal, C. J.; Macfarlane, R. D.; Thurston, E. L. *Anal. Chem.* **1979**, *51*, 2036–2039.
(20) Macfarlane, R. D.; Torgerson, D. F. *Science* **1976**, *191*, 920–925.
(21) Chait, B. T.; Agosta, W. C.; Field, F. H. *Int. J. Mass Spectrom. Ion Phys.* **1981**, *39*, 339–366.
(22) Lindsey, J. S.; Schreiman, I. C.; Hsu, H. C.; Kearney, P. C.; Marguerettaz, A. M. *J. Org. Chem.* **1987**, *52*, 827–836.
(23) Lindsey, J. S.; Wagner, R. W. *J. Org. Chem.* **1989**, *54*, 828–836.
(24) The lowest isotopic component (A + 0) contains all $^{12}C$, $^{14}N$, $^{16}O$; A + 1 contains one atom of $^{13}C$ with the remainder $^{12}C$, $^{14}N$, $^{16}O$, etc.
(25) McLafferty, F. W. *Interpretation of Mass Spectra*, 3rd ed.; University Science Books: Mill Valley, CA, 1980.
(26) Atamian, M.; Donohoe, R. J.; Lindsey, J. S.; Bocian, D. F. *J. Phys. Chem.* **1989**, *93*, 2236–2243.
(27) Collman, J. P.; Gagne, R. R.; Reed, C. A.; Halbert, T. R.; Lang, G.; Robinson, W. T. *J. Am. Chem. Soc.* **1975**, *97*, 1427–1439.
(28) Kathawalla, I. A.; Anderson, J. L.; Lindsey, J. S. *Macromolecules* **1989**, *22*, 1215–1219.

**Table I. Symmetric *meso*-Porphyrins**

| compd | aryl substituent (X) | position | formula | calcd | obsd |
|---|---|---|---|---|---|
| 1 | H | | $C_{44}H_{30}N_4$ | 614.2 | 614.3 |
| 2[a] | H | | $C_{44}H_{28}N_4Zn$ | 676.2 | 676.3 |
| 3 | H | | $C_{44}H_{30}{}^{15}N_4$ | 618.2 | 618.2 |
| 4 | $CH_3$ | 4 | $C_{48}H_{38}N_4$ | 670.3 | 670.2 |
| 5 | $CH_3$ | 2,4,6 | $C_{56}H_{54}N_4$ | 782.4 | 782.4 |
| 6 | $NO_2$ | 2 | $C_{44}H_{26}N_8O_8$ | 794.2 | 794.2 |
| 7 | $NH_2$ | 2 | $C_{44}H_{34}N_8$ | 674.3 | 674.4 |
| 8 | Ph | 4 | $C_{68}H_{46}N_4$ | 918.4 | 918.6 |
| 9 | $HOCH_2CH_2O$ | 4 | $C_{52}H_{46}N_4O_8$ | 854.3 | 854.5 |
| | | | | | 836.7[b] |
| 10 | dithiolane | 3 | $C_{56}H_{46}N_4S_8$ | 1030.1 | not res[c] |
| | | | | 1031.2 av | 1031.4 |
| 11 | dithiolane | 4 | $C_{56}H_{46}N_4S_8$ | 1030.1 | not res |
| | | | | 1031.2 av | 1031.4 |
| 12 | *n*-Bu-$O_2C$ | 4 | $C_{64}H_{62}N_4O_8$ | 1014.5 | 1014.6 |
| 13 | Phen$O_2C$ | 3 | $C_{80}H_{54}N_4O_{12}$ | 1262.4 | not res |
| | | | | 1263.2 av | 1262.8 |
| 14 | $CH_3O_2C$ | 4 | $C_{52}H_{38}N_4O_8$ | 846.3 | 846.3 |
| 15 | *t*-Bu$O_2C$ | 4 | $C_{64}H_{62}N_4O_8$ | 1014.5 | not res |
| | | | | 1015.1 av | 1015.6 |
| | | | | | 791.3[b] |
| 16 | NC | 4 | $C_{48}H_{26}N_8$ | 714.2 | 714.3 |
| 17 | $CH_2CHCH_2O$ | 4 | $C_{56}H_{46}N_4O_4$ | 838.4 | 838.5 |
| 18 | $-OCH_2O-$ | 3,4 | $C_{48}H_{30}N_4O_8$ | 790.2 | 790.3 |
| 19 | acetal | 4 | $C_{68}H_{70}N_4O_8$ | 1070.5 | 1070.9 |
| 20 | molecular cleft | 3 | $C_{92}H_{90}N_8O_{16}$ | 1562.6 | not res |
| | | | | 1563.7 av | 1564.4 |
| | | | | | 1586.7[d] |
| | | | | | 1608.7[d] |
| 21[a] | $CH_3(CH_2)_9O$ | 4 | $C_{84}H_{108}N_4O_4Zn$ | 1300.8 | not res |
| | | | | 1303.2 av | 1303.1 |
| 22 | Fmoc-Pro-NH | 4 | $C_{124}H_{102}N_{12}O_{12}$ | 1950.8 | not res |
| | | | | 1952.2 av | 1952.7 |
| 23 | $(CH_3)_3SiCC$ | 4 | $C_{64}H_{62}N_4Si_4$ | 998.4 | 998.3 |
| | porphine meso substituent (R) | | | | |
| 24 | $CH_3(CH_2)_4$ | | $C_{40}H_{54}N_4$ | 590.4 | 590.5 |
| 25 | $CH_3(CH_2)_9$ | | $C_{60}H_{94}N_4$ | 870.7 | 870.9 |
| 26 | $PhCH_2$ | | $C_{48}H_{38}N_4$ | 670.3 | 670.3 |
| 27 | PhCO | | $C_{48}H_{30}N_4O_4$ | 726.2 | 726.2 |

[a] Zinc chelate. [b] More intense than the molecule ion. [c] Not resolved. [d] Sodium-cationized species. Literature sources: **1, 9–14, 16–19, 24, 25**;[22] **3**;[26] **5**;[23] **6, 7**;[27] **8**;[28]; **20**;[29] **15, 21–23, 26, 27**;[30] compounds unspecified are available from commercial sources.

would yield a peak with approximately half the intensity of the A + 0 component. However, the observed peak at 671.2 u has an intensity fully 0.9 times that of the A + 0 peak, indicating the presence of protonated species $(M + H)^+$ in addition to the radical cation $M^{\bullet+}$. The peak at 671.2 u is attributed to the superposition of the A + 1 component of the $M^{\bullet+}$ species and the A + 0 component of the $(M + H)^+$ species. Nonetheless, the molecular ion ($M^{\bullet+}$) is clearly identifiable in the mass spectrum. The accuracy of mass analysis is high; the difference between the observed molecular mass and the calculated mass for the A + 0 component is only 0.1 u (Table I).

The mass spectrum of the zinc chelate of *meso*-tetraphenylporphyrin (**2**), is shown in Figure 2B. The spectrum exhibits a more complex pattern of peaks than the free base porphyrin (**1**) due to the three major isotopes of zinc ($^{64}Zn$, 48.6%; $^{66}Zn$, 27.9%; $^{68}Zn$, 18.8%). However, the lowest isotopic component (all $^{12}C$, $^{64}Zn$) is readily observable. As the mass of the porphyrin model compound increases, the individual components become more difficult to resolve. For example, the monoisotopic component of *meso*-tetrakis(4-(butoxycarbonyl)phenyl)porphyrin (**12**) (1014.6 u) can still be partially resolved from the higher components at 1015.5 and 1016.5 u (Figure 2C). A porphyrin bearing even larger substituents, such as the tetrakis(Fmoc-proline)porphyrin (**22**, Chart II), yields a mass spectrum without a resolved monoisotopic molecule ion peak (Figure 2D). Instead, an envelope is observed resulting from the superposition of isotopic components of the radical cation and protonated species. In this case, the calculated average mass for the radical cation is 1952.2 u and the observed mass is 1952.7 u (Table I). The peak of the envelope is shifted to higher mass than that calculated because of the admixture of protonated and radical cation species. The magnitude of this shift, in all cases studied, is at most 1 mass unit, although in general smaller shifts are observed (Table I). The peaks remain intense, and the loss of isotopic resolution does not greatly diminish the utility of the mass spectral method in confirming the identity of synthetic target compounds.

Almost all of the 100 compounds that we studied yielded a dominant intact ionized porphyrin peak. In a few cases fragment ions with intensities greater than that of the intact ionized molecule were observed, although the $M^{\bullet+}$ and/or the $(M + H)^+$ ion (which we collectively term the molecule ions) was always present in good yield. In a few other cases, sodium cationization of the molecule yielded higher mass peaks of greater intensity than the molecular ion. Those instances involving intense fragmentation or cationization are indicated below.

**2. Synthesis of Porphyrin–Quinone Compounds.** A cofacial porphyrin–quinone cage molecule was synthesized

(29) Lindsey, J. S.; Kearney, P. C.; Duff, R. J.; Tjivikua, P. T.; Rebek, J., Jr. *J. Am. Chem. Soc.* **1988**, *110*, 6575–6577.

(30) Unpublished results of J. S. Lindsey, T. E. Johnson, R. W. Wagner, and P. Sreedharan obtained at Rockefeller University and at Carnegie Mellon University.

**Chart II. A Selection of Substituents Appended to the Porphyrin Compounds**

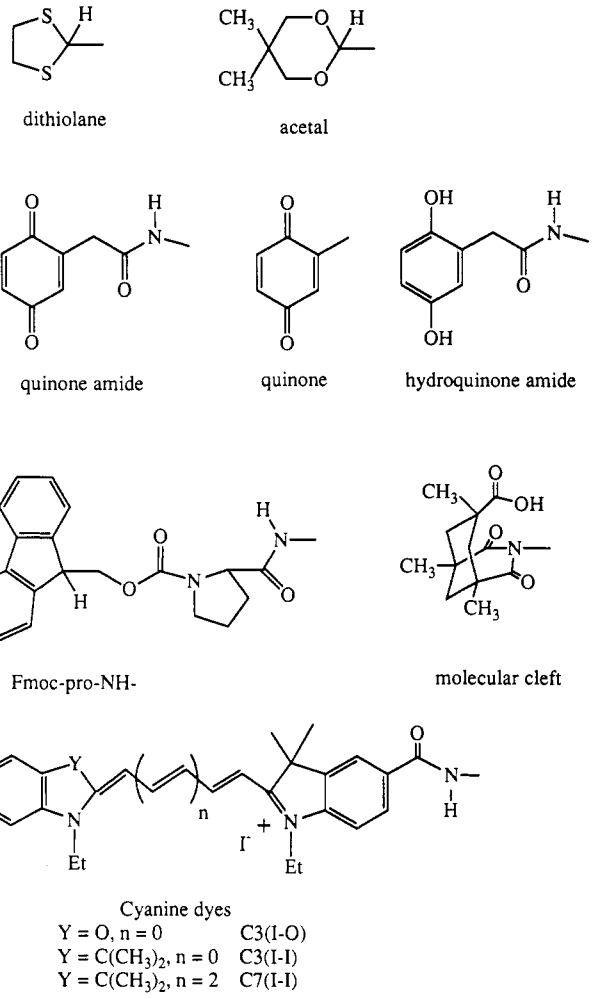


in order to examine photoinduced electron transfer reactions, as occur in the photosynthetic reaction centers.[31,32] A successful synthetic approach involved the condensation of a tetraaminoporphyrin with a tetraformyl quinone (Scheme I). The condensation was performed at room temperature with 0.5 mM porphyrin and quinone. Absorption spectroscopy of reaction aliquots taken over the course of 24 h showed the growing-in of a peak at 330 nm, indicative of Schiff base formation, but providing no distinction among possible intramolecularly-bonded (cage) and intermolecularly-linked (polymeric) porphyrin–quinone products.[33,34] A small sample of the crude reaction mixture (**28**), without purification, was analyzed by mass spectrometry (Figure 3). The peaks at 1367.1, 1384.9, and 1403.2 u are assigned to the porphyrin–quinone cage molecules with 4, 3, and 2 Schiff bases formed, respectively (Table II). These peaks can only derive from cage self-assembly, not intermolecular polymerization. The existence of these peaks indicated the porphyrin–quinone cage had formed; this incisive analysis encouraged subsequent studies of this promising self-assembly process.[34] Treatment of the porphyrin–quinone reaction mixture with $NaBH_3CN$ in order to reduce the Schiff bases gave rise to a new porphyrin component (**29**). Mass spectral analysis of this component confirmed that all four Schiff bases had been reduced as

**Scheme I. Self-Assembly of the Porphyrin–Quinone Cage Molecule PQ(4)[a]**

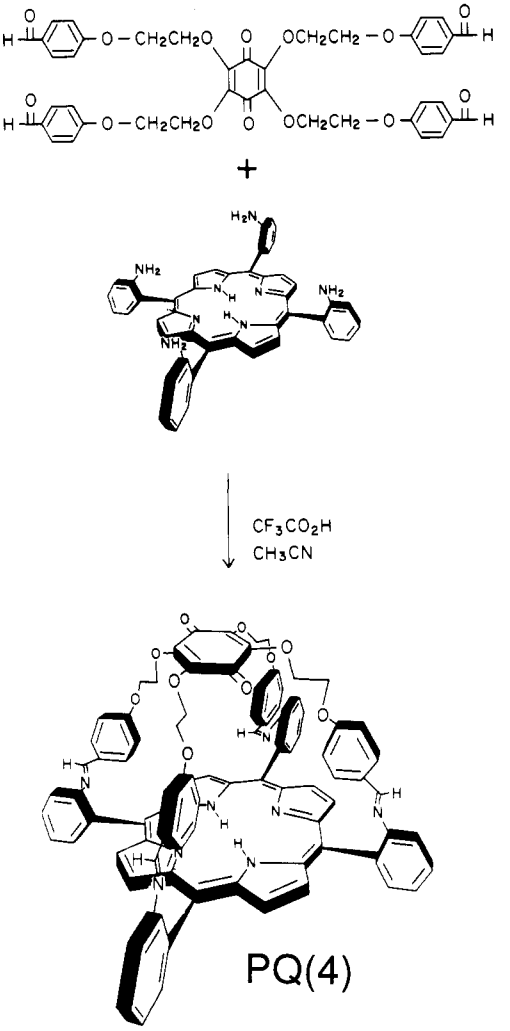


[a] The number, *n*, of Schiff bases formed is designated by PQ(*n*), where *n* = 1, 2, 3, or 4. Only PQ(4) is shown.

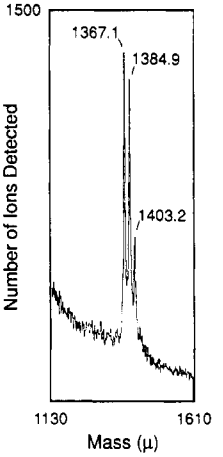


**Figure 3.** Partial mass spectrum of an unpurified sample (**28**) from the synthesis of a cofacial porphyrin–quinone, PQ(4).

evidenced by a peak at 1375.5 u, 8 mass units higher than the tetra-Schiff base product PQ(4), as expected (Table II). *We know of no other analytical method that provides such direct confirmation of the success of syntheses of this complexity.*

The mass spectral method proved equally valuable for assessing reactions involving modification of the porphyrin–quinones.[31] For example, the zinc–porphyrin–quinone (ZnPQ, **31**, Chart III, R = H, M = Zn) was treated with acetic

(31) Lindsey, J. S.; Delaney, J. K.; Mauzerall, D. C.; Linschitz, H. *J. Am. Chem. Soc.* **1988**, *110*, 3610–3621.
(32) Delaney, J. K.; Mauzerall, D. C.; Lindsey, J. S. *J. Am. Chem. Soc.* **1990**, *112*, 957–963.
(33) Lindsey, J. S.; Mauzerall, D. C. *J. Am. Chem. Soc.* **1982**, *104*, 4498–4500.
(34) Lindsey, J. S. *New J. Chem.* **1991**, *15*, 153–180.

**Table II. Porphyrin-Quinones**

| compd | | formula | calcd | obsd |
|---|---|---|---|---|
| 28 | PQ($n$) condensation[a] | | | |
| | PQ(4) | $C_{86}H_{62}N_8O_{10}$ | 1366.5 | not res |
| | | | 1367.4 av | 1367.1 |
| | PQ(3) | $C_{86}H_{64}N_8O_{11}$ | 1384.5 | not res |
| | | | 1385.5 av | 1384.9 |
| | PQ(2) | $C_{86}H_{66}N_8O_{12}$ | 1402.5 | not res |
| | | | 1403.5 av | 1403.2 |
| 29 | PQ | $C_{86}H_{70}N_8O_{10}$ | 1374.5 | not res |
| | | | 1375.5 av | 1375.5 |
| 30 | $PQH_2$ | $C_{86}H_{72}N_8O_{10}$ | 1376.5 | not res |
| | | | 1377.5 av | 1377.9 |
| 31[b] | ZnPQ | $C_{86}H_{68}N_8O_{10}Zn$ | 1436.4 | not res |
| | | | 1438.9 av | 1438.8 |
| 32[b] | $ZnPQ(Ac)_4$ | $C_{94}H_{76}N_8O_{14}Zn$ | 1604.5 | not res |
| | | | 1607.0 av | 1606.9 |
| | | | | 1629.6[c,d] |
| 33[b] | $ZnPA_4(Ac)_4$ | $C_{84}H_{72}N_8O_8Zn$ | 1384.5 | not res |
| | | | 1386.9 av | 1386.5 |
| 34[b] | $ZnPQ(palm)_2$ | $C_{118}H_{128}N_8O_{12}Zn$ | 1912.9 | not res |
| | | | 1915.6 av | 1915.2 |
| 35[b] | $ZnPQ(palm)_3$ | $C_{134}H_{158}N_8O_{13}Zn$ | 2151.1 | not res |
| | | | 2154.1 av | 2155.5 |
| | | | | 2177.4[c,e] |
| 36[b] | $ZnPQ(palm)_3(Ac)_1$ | $C_{136}H_{160}N_8O_{14}Zn$ | 2193.1 | not res |
| | | | 2196.1 av | 2196.2 |
| | | | | 2218.9[c,d] |
| 37 | chlorin–quinone $CQ_\alpha$ | $C_{86}H_{72}N_8O_{10}$ | 1376.5 | not res |
| | | | 1377.5 av | 1377.9 |
| 38 | chlorin–quinone $CQ_\beta$ | $C_{86}H_{72}N_8O_{10}$ | 1376.5 | not res |
| | | | 1377.5 av | 1377.8 |

[a] A sample from the crude reaction mixture was analyzed and found to contain PQ(4), PQ(3), and PQ(2) components. [b] Zinc chelate. [c] Sodium-cationized species. [d] More intense than the molecule ion. [e] Less intense than the molecule ion. Literature sources: **28**, **29**;[33] **30–33**, **37**, **38**;[31] **34–36**.[30]

anhydride in order to acylate the four amines in the bridging groups. Mass spectrometry was used to confirm that all four amines were acetylated (R = Ac). A complicating feature in the mass spectrum of $ZnPQ(Ac)_4$ (**32**) was the observation of a peak at 1629.6 u, which surpassed the molecular ion peak (1606.9 u) in intensity (Figure 4). The higher mass peak arose by $Na^+$ addition to the porphyrin. This effect was eliminated by soaking the sample foil in distilled water for 10 min.[35] Reanalysis of the sample showed the near total disappearance of the $Na^+$ addition peak and enhanced intensity of the molecular ion peak (Figure 4).

Other members of the porphyrin-quinone family were characterized with similar ease (Table II). In general, reaction products were examined by chromatography (TLC or HPLC), and purified components were analyzed by PDMS. However, even partially purified products (such as chromatography fractions) could be examined profitably in order to gain quick feedback concerning the success of a synthetic reaction. For example, ZnPQ (**31**) was treated with palmitic anhydride in an effort to prepare a tetrapalmitoyl derivative $ZnPQ(palm)_4$ that would be sufficiently amphipathic to orient spontaneously at the lipid–water interface. The amidation reaction was sluggish, and new porphyrin components were isolated by chromatography and characterized by PDMS (Table II). The products with two and three palmitoyl groups (**34**, **35**) were easily identified by the 238-u increment per added palmitoyl group. Prolonged treatment yielded a single component which upon mass spectral analysis was identified as $ZnPQ(palm)_3$ (**35**) rather than the expected $ZnPQ(palm)_4$. Because we sought to acylate all four amines, the product $ZnPQ(palm)_3$ was treated with excess acetic anhydride, forming $ZnPQ(palm)_3(Ac)_1$ (**36**) with characteristic peak at 2196.2 u (calcd av 2196.1 u) and with a more intense $Na^+$ addition peak at 2218.9 u (Table II).

(35) Aduru, S.; Chait, B. T. *Anal. Chem.* **1991**, *63*, 1621–1625.

**Chart III. Porphyrin-Quinone Derivatives $MPQ(R)_4$ and Related Porphyrin-Anisyl derivatives $MPA_4(R)_4$[a]**

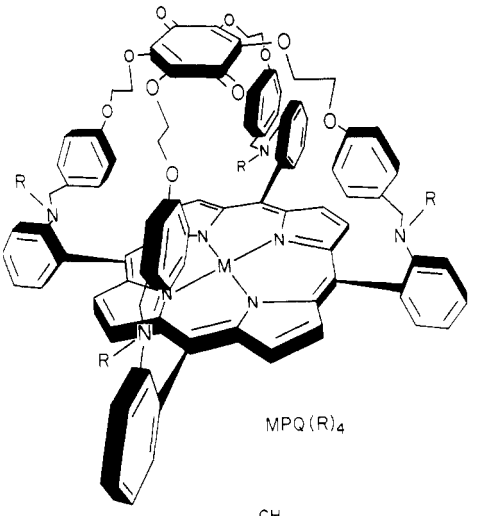


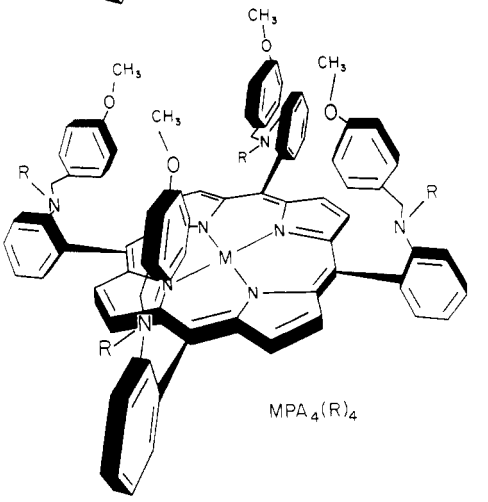


[a] The free base (M = H, H) porphyrin–quinone without derivatized bridge nitrogens (R = H) is designated PQ. Conversion of the quinone to the hydroquinone gives $PQH_2$. The zinc chelate, ZnPQ, can be acetylated (R = Ac), giving the tetraacetylated derivative, $ZnPQ(Ac)_4$. The porphyrin–tetraanisyl compound $PA_4$ and its derivatives are named in similar fashion.

In another series of experiments, the porphyrin–quinone (**29**) was treated with potassium azodicarboxylate to achieve reduction at the β-pyrrole positions, yielding the chlorin–quinone parallel and perpendicular isomers.[31] A number of products were formed in the reaction, requiring separation by HPLC. Absorption spectroscopy was used to distinguish chlorins from porphyrins and bacteriochlorins. Chlorin-containing fractions were then analyzed by PDMS to find which one contained the CQ isomers. The fraction that gave the CQ molecule ion (calcd av 1377.5 u) was subjected to further chromatography, ultimately resolving two closely-chromatographing components. Both exhibited typical chlorin absorption and fluorescence spectra. Upon mass spectral analysis, both components exhibited essentially identical molecule ion peaks (1377.9 u, 1377.8 u; calcd av 1377.5 u) and very similar fragmentation patterns, thus these components were necessarily the chlorin–quinone isomers (**37**, **38**) and not synthetic byproducts which contained the chlorin macrocycle (Table II). Insufficient material was obtained for $^1H$ NMR characterization; however, the sensitivity of PDMS and the ease of interpretation led to unambiguous identification of the chlorin–quinones.

**3. Synthetic Porphyrins.** We have prepared a diverse collection of porphyrins in exploring the scope of a new synthetic method for preparing porphyrins (Table I). Mass

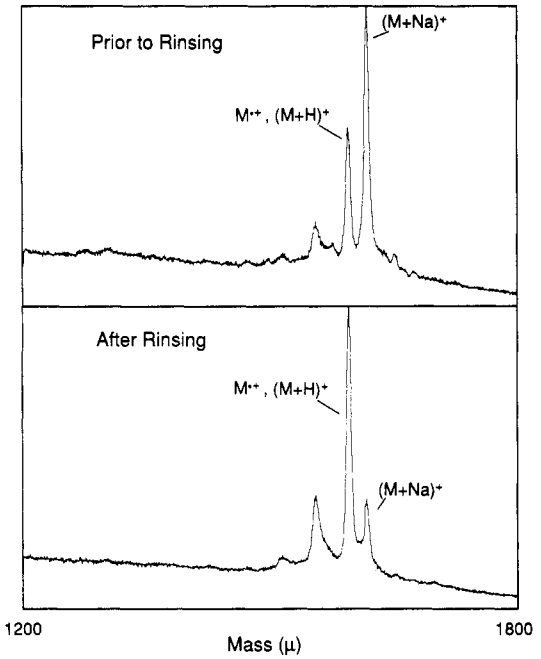


**Figure 4.** The mass spectrum of $ZnPQ(Ac)_4$ (**32**) shows $Na^+$ addition (top). After rinsing the sample film in water and reanalysis, the $Na^+$ is largely removed, yielding a more intense molecular ion peak.

## Chart IV. Facial and Peripheral Encumberance of the Porphyrin Achieved by 2,4,6-Trisubstitution of Each Phenyl Ring with Bulky Benzyloxy Groups[a]

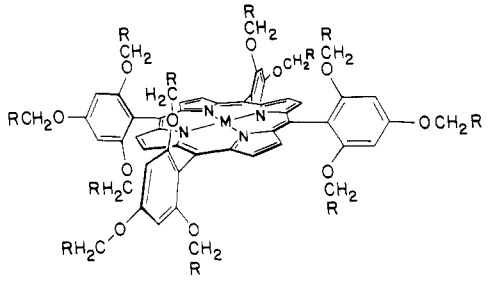

[a] Other substitution patterns include 2,6- or 3,5-disubstitution (not shown).

spectral analysis of the porphyrins yielded intense peaks corresponding to the intact ionized molecule, almost without regard to the molecular entities attached to the porphyrin macrocycle, making the interpretation of the spectra straightforward. Although information can be gleaned from examination of the fragmentation patterns, the presence of the intact molecule ion is sufficient to address the question of whether a porphyrin synthesis has proceeded as anticipated. Some examples included in Table I are particularly noteworthy. The molecular cleft porphyrin (**20**) underwent a small amount of sodium cationization but the molecule ion peak remained strong. The *tert*-butyl porphyrincarboxylate (**15**) yielded an intense fragment corresponding to the porphyrin carboxylic acid, but the molecule ion was still clearly observable. The *meso*-tetraalkylporphyrins (**24, 25**) undergo significant fragmentation at the $C_\alpha$–$C_\beta$ bond (vide infra), but the molecule ion peaks are intense, and the *meso*-alkylporphyrins are as amenable to mass spectrometric analysis as are the *meso*-arylporphyrins. The mass spectrometric method is also well-suited for characterizing isotopically-enriched porphyrins, such as $^{15}N$-TPP (**3**) (Table I).

*Facially-Encumbered Porphyrins.* A number of facially-encumbered porphyrins (Chart IV), prepared as components of a solid-state light-harvesting apparatus, were analyzed by

**Table III. Facially-Encumbered Porphyrins[36]**

| compd | R | position | formula | calcd | obsd |
|---|---|---|---|---|---|
| **39** | H | 2,6 | $C_{52}H_{46}N_4O_8$ | 854.3 | 854.4 |
| **40** | $C_6H_5$ | 2,6 | $C_{100}H_{78}N_4O_8$ | 1462.6 | not res |
| | | | | 1463.7 | 1464.1 |
| **41**[a] | $C_6H_5$ | 2,6 | $C_{100}H_{76}N_4O_8Zn$ | 1524.5 | not res |
| | | | | 1527.0 av | 1526.4 |
| **42** | $4\text{-}BrC_6H_4$ | 2,6 | $C_{100}H_{70}Br_8N_4O_8$ | 2085.9 | not res |
| | | | | 2094.9 av | 2094.9 |
| **43** | $4\text{-}CH_3C_6H_4$ | 2,6 | $C_{108}H_{94}N_4O_8$ | 1574.7 | not res |
| | | | | 1575.9 av | 1575.7 |
| **44** | $4\text{-}CH_3O_2CC_6H_4$ | 2,6 | $C_{116}H_{94}N_4O_{24}$ | 1926.6 | not res |
| | | | | 1928.0 av | 1928.1 |
| **45** | $C_6F_5$ | 2,6 | $C_{100}H_{38}F_{40}N_4O_8$ | 2182.2 | not res |
| | | | | 2183.3 av | 2183.0 |
| **46** | $C_6H_5$ | 3,5 | $C_{100}H_{78}N_4O_8$ | 1462.6 | not res |
| | | | | 1463.7 av | 1463.6 |
| **47** | $4\text{-}CH_3O_2CC_6H_4$ | 3,5 | $C_{116}H_{94}N_4O_{24}$ | 1926.6 | not res |
| | | | | 1928.0 av | 1927.8 |
| **48** | $C_6H_5$ | 2,4,6 | $C_{128}H_{102}N_4O_{12}$ | 1886.8 | not res |
| | | | | 1888.1 av | 1887.8 |
| **49** | $C_6F_5$ | 2,4,6 | $C_{128}H_{42}F_{60}N_4O_{12}$ | 2966.2 | not res |
| | | | | 2967.6 av | 2968.1 |

[a] Zinc chelate.

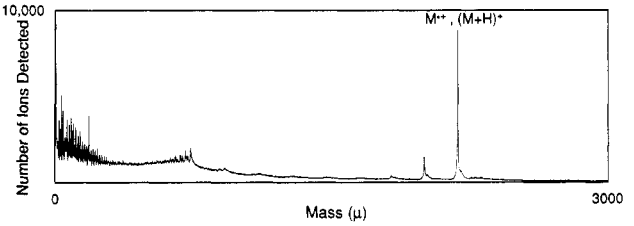


**Figure 5.** Mass spectrum of *meso*-tetrakis(2,6-bis((pentafluorobenzyl)-oxy)phenyl)porphyrin (**45**). The most intense peak in the mass spectrum is that of the molecule ion, in spite of the fact that the porphyrin skeleton ($C_{20}H_{10}N_4$, 306 u) comprises only 15% of the total mass (2182.2 u).

mass spectrometry (Table III).[36] The presence of 8 or 12 benzyloxy groups attached to the porphyrin gives molecular weights in the 1400–3000 range (**40–49**). Surprisingly, the projection of bulky benzyloxy groups over the face of the porphyrin does not impede analysis by mass spectrometry, in spite of the fact that in the bulkiest compounds the porphyrin chromophore only constitutes 10–20% of the total mass. Indeed, this family of porphyrins yielded intense molecule ion peaks in 2–30-min runs as easily as porphyrins without facial encumberance. The octakis- and dodecakis-(benzyloxy)porphyrins underwent significantly more fragmentation than the simpler octamethoxyporphyrin (**39**), but the fragmentation yielded a broad spectrum of nondistinct peaks of lesser intensity than the molecule ion peak, thus not interfering with a clear identification of the intact molecular ion (Figure 5). A particularly interesting porphyrin is the octabromo derivative (**42**). Although the calculated A + 0 mass is 2085.9, the isotopes of bromine result in a calcd av mass of 2094.9 u (Table III). The apex of the experimental peak was measured at 2094.9 u.

*Hybrid Porphyrins.* The condensation of two aldehydes (A and B) with pyrrole, in principle, yields four hybrid porphyrins ($AB_3$, cis and trans $A_2B_2$, and $A_3B$) and the two parent porphyrins ($A_4$ and $B_4$). In general the chromatographic elution order of the porphyrins occurs in accord with the differing polarities of the two aldehydes used in the mixed aldehyde condensation. Mass spectrometry was used to confirm the identity of the porphyrins isolated by chroma-

(36) Wagner, R. W.; Breakwell, B. V.; Ruffing, J.; Lindsey, J. S. *Tetrahedron Lett.* **1991**, *32*, 1703–1706.
(37) Atamian, M.; Wagner, R. W.; Lindsey, J. S.; Bocian, D. F. *Inorg. Chem.* **1988**, *27*, 1510–1512.

**Table IV. Hybrid Porphyrins**

| compd | porphine meso substituents (R) 5 | 10 | 15 | 20 | formula | calcd | obsd |
|---|---|---|---|---|---|---|---|
| | | | Alkyl–Aryl and Phenyl–Aryl Hybrid Porphyrins | | | | |
| **50** | Ph | Ph | Ph | Ar | $C_{46}H_{32}N_4O_2$ | 672.3 | 672.1 |
| **51** | Ar | Ph | Ar | Ph | $C_{48}H_{34}N_4O_4$ | 730.3 | 730.2 |
| **52** | Ar | Ar | Ph | Ph | $C_{48}H_{34}N_4O_4$ | 730.3 | 730.2 |
| **53** | Ar | Ar | Ar | Ph | $C_{50}H_{36}N_4O_6$ | 788.3 | 788.2 |
| **54** | Ar | Ar | Ar | *n*-pentyl | $C_{49}H_{42}N_4O_6$ | 782.3 | 782.3 |
| **55** | *n*-pentyl | Ar | *n*-pentyl | Ar | $C_{46}H_{46}N_4O_4$ | 718.4 | 718.4 |
| **56** | *n*-pentyl | *n*-pentyl | Ar | Ar | $C_{46}H_{46}N_4O_4$ | 718.4 | 718.4 |
| **57** | *n*-pentyl | *n*-pentyl | *n*-pentyl | Ar | $C_{43}H_{50}N_4O_2$ | 654.4 | 654.5 |
| **58** | $C_6H_5CO$ | *p*-tolyl | *p*-tolyl | *p*-tolyl | $C_{48}H_{36}N_4O$ | 684.3 | 684.3 |
| **59** | $PhCH_2CH_2$ | Ph | Ph | Ph | $C_{46}H_{34}N_4$ | 642.3 | 642.4<br>551.2[d] |
| | | | Monofunctionalized Porphyrins | | | | |
| | 5 | 10,15,20 | | | | | |
| | 4-aryl substituents (X) | meso substituents (R) | | | | | |
| **60**[a] | cyanine C3(I–O) | Ph | | | $C_{69}H_{56}N_7O_2$ | 1014.5<br>1015.1 av | not res<br>1015.3 |
| **61**[a] | cyanine C3(I–I) | Ph | | | $C_{72}H_{62}N_7O$ | 1040.5<br>1041.2 av | not res<br>1041.4 |
| **62**[a] | cyanine C7(I–I) | Ph | | | $C_{76}H_{66}N_7O$ | 1092.5<br>1093.3 av | not res<br>1093.4 |
| **63** | $ClCH_2CONH$ | Ms | | | $C_{55}H_{50}ClN_5O$ | 831.4 | 831.3 |
| **64** | $PhthCH_2$ | Ms | | | $C_{62}H_{53}N_5O_2$ | 899.4 | 899.4 |
| **65**[b,c] | $H_2N$ | Ph | | | $C_{44}H_{29}N_5Zn$ | 691.2 | 691.2 |
| **66** | $CH_3O_2C$ | Ms | | | $C_{55}H_{50}N_4O_2$ | 798.4 | 798.3 |
| **67** | $(CH_3)_3Si(CH_2)_2O_2C$ | Ms | | | $C_{59}H_{60}N_4O_2Si$ | 884.4 | 884.4 |
| **68** | $HO_2C$ | Ms | | | $C_{54}H_{48}N_4O_2$ | 784.4 | 784.3 |
| **69** | $HO_2CCH(CH_3)NHCO$ | Ms | | | $C_{57}H_{53}N_5O_3$ | 855.4 | 855.4 |
| **70** | Fmoc-Pro-NH | Ms | | | $C_{73}H_{66}N_6O_3$ | 1074.5 | 1074.5 |
| **71** | H-Pro-NH | Ms | | | $C_{58}H_{56}N_6O$ | 852.5<br>853.0 av | not res<br>853.5 |
| **72**[b] | $c\text{-}C_5H_{10}NCO$ | Ms | | | $C_{59}H_{55}N_5OZn$ | 913.4 | 913.4 |
| **73** | $SuO_2C$ | Ph | | | $C_{49}H_{33}N_5O_4$ | 755.3 | 755.4 |
| **74** | dithiolane | *n*-pentyl | | | $C_{44}H_{52}N_4S_2$ | 700.4 | 700.4 |
| **75** | $PhenO_2C$ | *n*-decyl | | | $C_{65}H_{84}N_4O_3$ | 968.7 | 968.7 |
| **76** | $(CH_3)_3SiCC$ | $2,4,6\text{-}MeO_3C_6H_2$ | | | $C_{58}H_{56}N_4O_9Si$ | 980.4 | 980.3 |
| **77** | $(CH_3)_2N$ | $C_6F_5$ | | | $C_{46}H_{20}F_{15}N_5$ | 927.1 | 927.2 |
| **78** | quinone amide | *p*-tolyl | | | $C_{55}H_{41}N_5O_3$ | 819.3 | 819.3 |
| **79** | hydroquinone amide | *p*-tolyl | | | $C_{55}H_{43}N_5O_3$ | 821.3 | 822.3 |
| **80**[b] | quinone amide | *p*-tolyl | | | $C_{55}H_{39}N_5O_3Zn$ | 881.2 | 881.4 |
| **81** | quinone | Ph | | | $C_{50}H_{32}N_4O_2$ | 720.3 | 720.4 |
| | | | Multifunctionalized Porphyrins | | | | |
| | 5 | 10,15,20 | | | | | |
| | 4-aryl substituents (X) | 4-aryl substituents (X) | | | | | |
| **82** | Fc- | quinone | | | $C_{72}H_{44}N_4O_6Fe$ | 1116.3<br>1117.0 av | not res<br>1117.9 |
| **83** | t-Bu-$O_2C$- | Fmoc-Pro-NH | | | $C_{109}H_{92}N_{10}O_{11}$ | 1716.7<br>1717.9 av | not res<br>1718.8[e] |
| **84** | $HO_2C$- | Fmoc-Pro-NH | | | $C_{105}H_{84}N_{10}O_{11}$ | 1660.6<br>1661.8 av | not res<br>1662.3 |

[a] The formula and calculated masses are for the porphyrin–dye cation without a counterion. [b] Zinc chelate. [c] Ortho substituted, not para. [d] More intense than the molecule ion. [e] May be protonated. Abbreviations: Su, succinimidyl; Phen, phenacyl; Phth, phthalimido; Fc, ferrocenyl. Literature sources: **50–57**;[37] **58–59, 63, 64, 66–84**;[30] **65**;[31] **60–62**.[38]

tography (for aldehydes with different molecular weights), although no mass spectral distinction was possible for the cis- and trans-disubstituted porphyrins. The mass spectrometric method was successfully applied to porphyrins bearing a wide variety of groups, including carboxylic acids, protected amino acids, active esters, dithioacetals, aromatic amines, quinone, ferrocene, and trimethylsilyl protecting groups (Table IV). The clear distinction observed between porphyrin–quinone (**78**) and porphyrin–hydroquinone (**79**) molecules, in spite of the only 2-u mass difference, enabled the ferreting out of reduced (**79**) and oxidized (**78**) species from crude reaction mixtures.

Porphyrins bearing *meso*-alkyl groups undergo fragmentation at the $C_\alpha$–$C_\beta$ bond, often forming fragment ion peaks of greater intensity than that of the porphyrin molecular ion. This fragmentation pattern mirrors the well-known benzylic fragmentation of $\beta$-pyrrole substituted porphyrins.[1,2] In a series of pentyl–aryl hybrid porphyrins (Table IV), the monopentylporphyrin (**54**) gave a molecular ion (782.3 u) and a single fragment at 725.2 u; the latter derives from benzyl-like cleavage of the $C_\alpha$–$C_\beta$ bond and loss of a butyl fragment. Similarly, the cis and trans porphyrins (**55, 56**), the tripentylporphyrin (**57**), and the tetrapentylporphyrin (**24**) each gave a molecular ion peak and fragments due to successive loss of two, three, and four substituents, respectively. The monophenethylporphyrin (**59**) undergoes $C_\alpha$–$C_\beta$ cleavage to yield two benzylic fragments. The high-mass fragment (porphyrin – benzyl (551.2 u)) was the most intense peak in the spectrum (with the exception of that of $H^+$), and the second most intense peak was due to the porphyrin molecular ion (642.4 u). The occurrence of fragmentation does not greatly complicate the interpretation, and in no cases have

we observed fragmentation of such intensity that the molecular ion could not easily be identified.

Several porphyrin cyanine dyes (**60–62**) were prepared as model systems for visible light harvesting (Chart II).[38] The cyanine dyes are ionic, consisting of a cationic organic dye and an anionic counterion. Though the initial counterion in the synthesis was iodide, ion exchange during normal handling can lead to a final product with several different counterions, potentially complicating analysis by NMR spectroscopy. Mass spectrometry cleanly sidesteps this pitfall because the negatively-charged counterions are not detected in the positive ion spectra. Each of the porphyrin cyanine dyes (**60–62**) gave a strong ion peak consistent with the calculated average mass of the porphyrin cyanine dye minus a counterion (Table IV). The mass spectra were readily interpreted, thus confirming the success of the synthesis. In contrast, the $^1$H NMR spectra proved extremely difficult to interpret due to the large number of distinct protons in the asymmetric porphyrin and asymmetric cyanine dye. Further complications of interpretation were attributed to ion pairing of several different counterions with the cationic dyes in the nonpolar NMR solvents.

The porphyrin–indotricarbocyanine dye (**62**) gave a molecular ion peak at 1093.4 u, a fragment peak of lesser intensity at 556.6 u, and the intervening spectral region was almost devoid of peaks. The peak at 556.6 u derives from cleavage of the porphyrin–phenyl C–C bond, yielding the charged dye fragment ($C_{38}H_{41}N_3O$). A smaller fragment peak at 546.7 u (half the mass of the molecular ion) may arise from the doubly charged molecular ion. The cyanine dye bears one intrinsic positive charge, and ionization of the porphyrin would yield the doubly charged molecule. For the carbocyanine dye–porphyrins (**60, 61**), no peaks characteristic of the doubly-charged molecular ion were detected that were of greater intensity than fragments in the appropriate spectral region.

*Strapped Porphyrins.* The positioning of straps across adjacent *meso*-phenyl groups represents an attractive architecture for porphyrin model systems. We prepared a series of strapped porphyrins (Chart V) in order to study the effect of strap structure on porphyrin formation, as well as to obtain porphyrins bearing redox-active groups.[39] The porphyrins with straps at the ortho positions form atropisomers (with the two straps on the same face or on opposite faces of the porphyrin) which are separable chromatographically. The meta-strapped porphyrins can form atropisomers in principle, but in practice we have only observed one meta-strapped porphyrin chromatographic component in the synthesis of each meta-strapped porphyrin.[39] The $^1$H NMR spectra of the meta-strapped porphyrins are complicated, apparently due to the slow interconversion of the atropisomers. Variable-temperature NMR experiments were performed to investigate the interconversion processes, but given the complexity of the spectra and the dynamics of the molecular processes (which differed depending on the nature of the strap), NMR spectroscopy was not very potent for providing confirmation that the syntheses had succeeded.

Mass spectrometry played a crucial role in the characterization of the strapped porphyrins (Table V). In the spectra of the *o*- and *m*-alkoxy-strapped porphyrins (**85–93**), peaks of low intensity were frequently observed at masses two, three, and $^3/_2$ times that of the molecular ion. These are attributed to the singly-charged dimer, the singly-charged trimer, and the doubly-charged trimer of porphyrins, respectively. A small amount of noncovalent dimer formation is frequently observed with porphyrins upon mass spectral analysis, but

**Chart V. Strapped Porphyrins**[a]

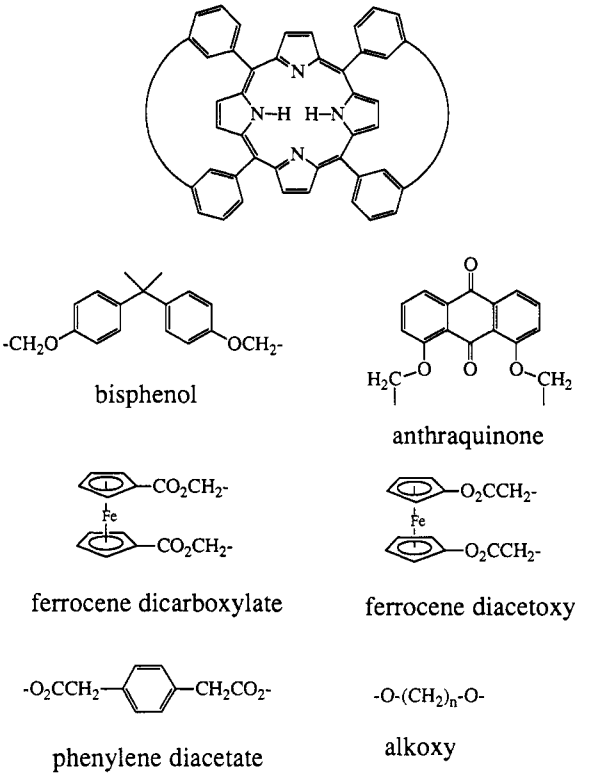


[a] The straps that are shown span the meta positions of adjacent phenyl groups. Only the alkoxy chain has been used to span ortho positions (not shown).

these are the only examples, to our knowledge, of noncovalent trimers formed from tetraphenylporphyrins. The prevalence of these higher mass peaks was in accord with the poor solubility of the *o*- and *m*-alkoxy-strapped porphyrins. In two cases (meta-$C_5$ (**89**), meta-$C_7$ (**91**)) we observed higher mass components (+312.7 u, +340.7 u, respectively) that could be attributed to the monostrapped porphyrin with two free aldehyde groups (identical in architecture to the cis-$Ar_2$-monostrapped porphyrins, Chart VI, and formed by failure to close the second strap). Though the intensity of these peaks was low (~10% of the molecular ion), their presence led us to reevaluate the synthetic method and purification procedures.

Hybrid-strapped porphyrins (**99–101**) also were prepared by condensing two different linked dialdehydes, yielding, for example, a strapped porphyrin (**101**) bearing a ferrocene in one strap and an anthraquinone in the other strap (Table V).[39] The observation of an intense peak at 1177.3 u coincided with the calculated average mass of 1177.0 u for the ferrocene–porphyrin–quinone (**101**), providing quick confirmation of the successful synthesis and isolation of the desired target. Similar mixed aldehyde condensations were performed in the synthesis of cis-disubstituted porphyrins (Chart VI). The mass spectra (Table V) provided unambiguous identification of the target molecules.

**4. Porphyrin–Porphyrin Dimers.** A building block approach was exploited to prepare porphyrin–porphyrin dimers for studies of visible light harvesting (Chart VII). Coupling of a monocarboxyporphyrin with a monoprolylporphyrin (**71**) yielded a number of chromatographic components. Analysis by mass spectrometry of each major component readily identified the component consisting of the zinc porphyrin/free base porphyrin dimer (**113**, Table VI). The mass spectrum showed a peak due to the dimer at 1683.1 u (calcd av mass, 1683.4 u) and a sizeable fragment peak at 803.3 u (Figure 6). The latter is easily assigned to the fragment

(38) Lindsey, J. S.; Brown, P. A.; Siesel, D. A. *Tetrahedron* **1989**, *45*, 4845–4866.
(39) Wagner, R. W.; Brown, P. A.; Johnson, T. E.; Lindsey, J. S. *J. Chem. Soc., Chem. Commun.* **1991**, 1463–1466.

**Table V. Strapped Porphyrins**

| compd | position | formula | calcd | obsd |
|---|---|---|---|---|
| | | $-O(CH_2)_nO-$ Straps | | |
| ortho straps | *n* | | | |
| 85 | 5 | $C_{54}H_{46}N_4O_4$ | 814.4 | 814.4 |
| 86 | 7 | $C_{58}H_{54}N_4O_4$ | 870.4 | 870.5 |
| 87 | 8 | $C_{60}H_{58}N_4O_4$ | 898.4 | 898.6 |
| 88 | 10 | $C_{64}H_{66}N_4O_4$ | 954.5 | 955.4 |
| meta straps | *n* | | | |
| 89 | 5 | $C_{54}H_{46}N_4O_4$ | 814.4 | 814.4 |
| 90 | 6 | $C_{56}H_{50}N_4O_4$ | 842.4 | 842.4 |
| 91 | 7 | $C_{58}H_{54}N_4O_4$ | 870.4 | 870.4 |
| 92 | 8 | $C_{60}H_{58}N_4O_4$ | 898.4 | 898.4 |
| 93 | 10 | $C_{64}H_{66}N_4O_4$ | 954.5 | 954.6 |
| meta straps | name | | | |
| 94 | bisphenol | $C_{78}H_{62}N_4O_4$ | 1118.5 | not res |
| | | | 1119.3 av | 1119.6 |
| 95[a] | bisphenol | $C_{78}H_{60}N_4O_4Zn$ | 1180.4 | not res |
| | | | 1182.7 av | 1182.4 |
| 96 | phenylenediacetate | $C_{68}H_{50}N_4O_8$ | 1050.4 | 1050.5 |
| 97 | ferrocenedicarboxylate | $C_{72}H_{50}N_4O_8Fe_2$ | 1210.2 | not res |
| | | | 1210.8 av | 1211.7 |
| 98 | ferrocene diacetoxy | $C_{72}H_{50}N_4O_8Fe_2$ | 1210.2 | not res |
| | | | 1210.8 av | 1211.8 |

| compd | strap 1 | strap 2 | formula | calcd | obsd |
|---|---|---|---|---|---|
| | | Hybrid-Strapped Porphyrins (All Meta) | | | |
| 99 | ferrocenedicarboxylate | $-O(CH_2)_8O-$ | $C_{66}H_{54}N_4O_6Fe$ | 1054.3 | not res |
| | | | | 1054.9 av | 1055.0 |
| 100 | anthraquinone | $-O(CH_2)_8O-$ | $C_{68}H_{52}N_4O_6$ | 1020.4 | 1020.5 |
| 101 | ferrocenedicarboxylate | anthraquinone | $C_{74}H_{48}N_4O_8Fe$ | 1176.3 | not res |
| | | | | 1177.0 av | 1177.3 |

| $-O(CH_2)_nO-$ strap | | | $4\text{-}ZC_6H_4$ | | | |
|---|---|---|---|---|---|---|
| compd | *n* | position | (Z) | formula | calcd | obsd |
| | | | Cis-$Ar_2$-Strapped Porphyrins | | | |
| 102 | 5 | ortho | $CH_3O_2C$ | $C_{53}H_{42}N_4O_6$ | 830.3 | 830.3 |
| 103[a] | 5 | ortho | $CH_3O_2C$ | $C_{53}H_{40}N_4O_6Zn$ | 892.2 | 892.4 |
| 104 | 5 | ortho | $CH_3(CH_2)_7O$ | $C_{65}H_{70}N_4O_4$ | 970.5 | 970.6 |
| 105 | 5 | ortho | $(CH_3)_2N$ | $C_{53}H_{48}N_6O_2$ | 800.4 | 800.6 |
| 106 | 8 | meta | $CH_3O_2C$ | $C_{56}H_{48}N_4O_6$ | 872.4 | 872.4 |

[a] Zinc chelate. Literature sources: 85–101;[39] 102–106.[30]

**Chart VI. Porphyrins Bearing a Single Strapping Unit and Cis-Substituted Z Groups (for Substituent Z, See Table V)**

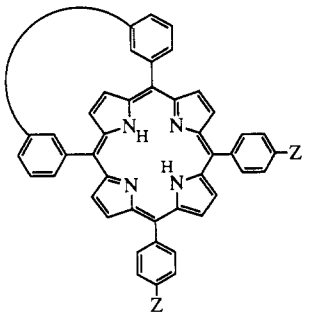


derived from cleavage at the carbonyl–phenyl bond, liberating the zinc–trimesitylmonophenylporphyrin fragment ($C_{53}H_{45}N_4Zn$, calcd av 803.3 u). Similarly, the free base porphyrin/free base porphyrin dimer (**114**) fragmented at the same bond site, yielding a fragment at 740.1 u ($C_{53}H_{47}N_4$, calcd av 739.9 u; data not shown). The region between the molecule ion and the major fragment peak was almost devoid of peaks in both spectra, rendering the analysis very straightforward. The free base/free base porphyrin dimer (**114**) was analyzed on a nitrocellulose layer[40,41] rather than aluminized Mylar, but no decrease in the extent of fragmentation was detected.

Porphyrin–porphyrin dimers (**107–112**) in a gable-type configuration[42] incorporating zinc, iron, or manganese were also analyzed by PDMS (Table VI). Sample preparation and analysis in PDMS are sufficiently mild that porphyrin demetalation does not occur. The biszinc chelate (**108**) was prepared with the bridging ligands dipyridylmethane or 1,3-bis(*N*-imidazolyl)propane. The mass spectra of these bisporphyrin complexes gave the molecule ion with loss of the linker, and in both cases the peak due to the protonated linker (dipyridylmethane, 171.0; bis(imidazolyl)propane, 177.0) was observed. The manganese and iron chelates each have a fifth ligand site, which in the bisporphyrins was occupied by chloride. The mass spectra of the bismanganese chelate (**109**) showed no molecule ion; instead molecule ions with loss of one and two chloride atoms were observed. The bisiron chelate (**110**) gave an observable molecule ion, but the peaks due to loss of one and two chloride atoms were more intense (Figure 7). However, each component in the cluster of peaks

(40) Jonsson, G. P.; Hedin, A. B.; Hakansson, P. L.; Sundqvist, B. U. R.; Save, B. G. S.; Nielsen, P. F.; Roepstorff, P.; Johansson, K. E.; Kamensky, I.; Lindberg, M. S. L. *Anal. Chem.* **1986**, *58*, 1084–1087.

(41) Chait, B. T. *Int. J. Mass Spectrom. Ion Processes* **1987**, *78*, 237–250. Chait, B. T.; Field, F. H. *Biochem. Biophys. Res. Commun.* **1986**, *134*, 420–426.

(42) Tabushi, I.; Sasaki, T. *Tetrahedron Lett.* **1982**, *23*, 1913–1916. Tabushi, I.; Kugimiya, S.; Kinnaird, M. G.; Sasaki, T. *J. Am. Chem. Soc.* **1985**, *107*, 4192–4199.

(43) Unpublished results of T. Sasaki and I. Tabushi obtained at Kyoto University.

**Table VI. Porphyrin Dimers**

| compd | $Ar_1$ | $Ar_2$ | spacer | $rM_1$ | $M_2$ | formula | calcd | obsd |
|---|---|---|---|---|---|---|---|---|
| | | | | Gable Porphyrins[a] | | | | |
| 107 | Ph | Ph | gable | H,H | H,H | $C_{82}H_{54}N_8$ | 1150.4 | 1150.3 |
| 108 | Ph | Ph | gable | Zn | Zn | $C_{82}H_{50}N_8Zn_2$ | 1274.3 | not res |
| | | | | | | | 1278.1 av | 1278.4 |
| 109 | Ph | Ph | gable | Mn-Cl | Mn-Cl | $C_{82}H_{50}N_8Mn_2Cl_2$ | 1326.2 | not res |
| | | | | | | | 1327.9 av | no molecule ion |
| | | | | | | | | 1292.9 (2) |
| | | | | | | | | 1257.2 (1) |
| 110 | Ph | Ph | gable | Fe-Cl | Fe-Cl | $C_{82}H_{50}N_8Fe_2Cl_2$ | 1328.2 | not res |
| | | | | | | | 1329.7 av | 1330.0 (4) |
| | | | | | | | | 1294.5 (2) |
| | | | | | | | | 1259.1 (1) |
| | | | | | | | | 1181.6 (3) |
| | | | | | | | | 1103.3 (5) |
| 111 | Ph | *p*-tolyl | gable | H,H | H,H | $C_{85}H_{60}N_8$ | 1192.5 | not res |
| | | | | | | | 1193.4 av | 1193.6 |
| 112 | Ph | *p*-tolyl | gable | Fe-Cl | Fe-Cl | $C_{85}H_{56}N_8Fe_2Cl_2$ | 1370.3 | not res |
| | | | | | | | 1371.8 av | 1371.8 (3) |
| | | | | | | | | 1336.8 (2) |
| | | | | | | | | 1301.4 (1) |
| | | | | Building Block Porphyrin Dimers | | | | |
| 113 | Ms | Ms | proline | Zn | H,H | $C_{112}H_{100}N_{10}O_2Zn$ | 1680.7 | not res |
| | | | | | | | 1683.4 av | 1683.1 |
| 114 | Ms | Ms | proline | H,H | H,H | $C_{112}H_{102}N_{10}O_2$ | 1618.8 | not res |
| | | | | | | | 1620.0 av | 1620.2 |
| 115 | Ar[c] | Ar[c] | alkyne | H,H | H,H | $C_{102}H_{80}N_8O_{12}Zn$ | 1672.5 | not res |
| | | | | | | | 1675.1 av | 1675.0 |

[a] The gable porphyrins were prepared by Professor Tomikazu Sasaki (University of Washington). [b] The numbers in parentheses indicate the relative order of intensity of the peaks. [c] Ar = 2,6-$(MeO)_2C_6H_3$. Literature sources: **107, 108, 110–112;**[42] **109;**[43] **113–115.**[30]

**Chart VII. Porphyrin Dimers with Various Spacers and Differential Metalation ($M_1$, $M_2$)[a]**

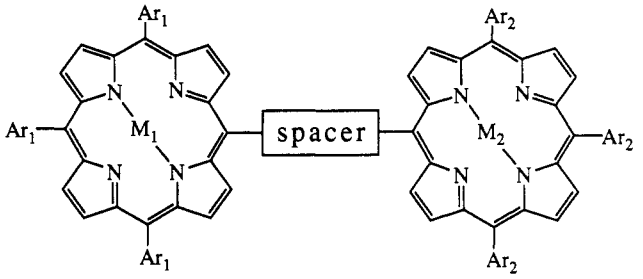


spacers

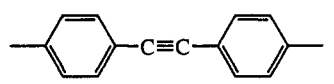


alkyne

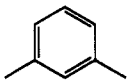

gable

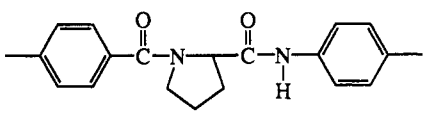


proline

[a] The gable porphyrins were prepared by Tabushi, Sasaki and co-workers.[42]

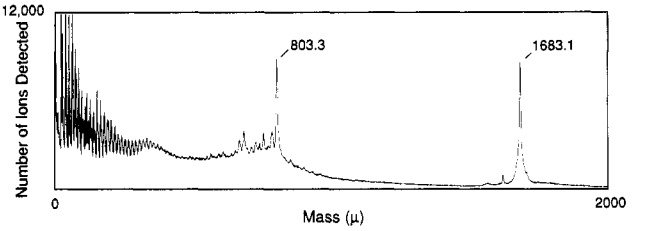


**Figure 6. The mass spectrum of a porphyrin–porphyrin dimer (113) shows the intact molecule ion peak (1683.1 u) and a sizeable fragment peak (803.3 u). The lower mass fragments exhibit the characteristic oscillation of intensity with a 14-u periodicity.**

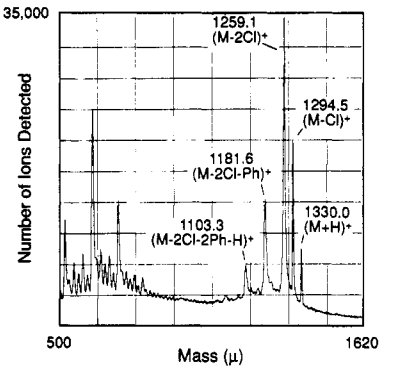


**Figure 7. The mass spectrum of a gable porphyrin (110) shows several peaks clustered near the molecule ion, due to loss of ligands bound to the metals.**

was readily assigned to fragments derived from loss of chloride or phenyl moieties, not demetalation of the porphyrin.

## CONCLUSIONS

$^{252}Cf$ PDMS is applicable to porphyrin model systems spanning an enormous range of architectures and functional group diversity. The method is especially well-suited for characterizing chromatographic fractions and partially purified components, thereby allowing reactions to be easily followed. The mass spectra are collected quickly and are readily interpreted, enabling rapid feedback concerning the outcome of a synthetic reaction. Taken together, these features make this method an extremely powerful tool for research in the synthesis of bioorganic porphyrin model systems. Our experience with porphyrin model systems leads us to believe that similar strategies employing $^{252}Cf$ PDMS

would accelerate progress in many other areas of synthetic organic chemistry.

## ACKNOWLEDGMENT

This work was supported by NIH grants to J.S.L (GM-36238) and to B.T.C. (RROO 862) and by the Rockefeller University Graduate Program. The spectra were collected at The Rockefeller University Mass Spectrometric Biotechnology Research Resource, which is supported in part by the Division of Research Resources, National Institutes of Health. We thank Tomikazu Sasaki (University of Washington) for permission to show the data of the gable porphyrins.

RECEIVED for Review May 27, 1992. Accepted July 31, 1992.